Journal of Power Sources, *33* (1991) 187–212

Variables affecting the deep-cycling characteristics of expanded-grid lead/acid battery plates

E. M. L. Valeriote* and **A. Heim**
Cominco Product Technology Centre, Sheridan Park, Mississauga, Ont., L5K 1B4 (Canada)
M. S. Ho
62 Signature Close, Calgary, Alta., T3H 2V7 (Canada)

Abstract

A large number of experimental lead/acid cells have been constructed, cycled, and examined using metallographic techniques in order to evaluate the influence of cell fabrication and operating variables on capacity retention. The effects of grid alloy (especially tin and calcium contents in expanded grids), extent of recharge, processing variables, additives and other parameters have been investigated and some of the results are presented here. Under the experimental conditions, long cycle-lives have been obtained, without any rapid or premature capacity loss for non-antimonial alloys, regardless of the presence or absence of tin in the grid alloy. The main influence of tin appeared to be related to the corrosion and growth characteristics of the grid. With 115% constant-current recharge, cell failures for certain grid alloys (e.g., low-calcium, high-tin lead alloys) were due to corrosion and wire breakage. For preferred alloys, and at 105% recharge, capacity losses were brought about by less obvious factors. The latter were apparently related to grid growth, active material degradation, and/or loss of electrical continuity with the current collector. Some evidence has been found for the formation of $PbSO_4$ and α-PbO in the corrosion layer; this may have contributed to performance degradation. Neither of these lead species, however, appeared to form a continuous barrier in recharged plates or to cause sudden capacity loss. The charging regime chosen was suitable to ensure good cycle-life regardless of tin content and some of the other variables studied. A different cycling regime and state-of-charge for plate removal and examination is required in order to study corrosion-layer passivation, which was largely absent in this work.

Introduction

During the 1970s, the incorporation of lead–calcium (PbCa) alloy grids into lead/acid automotive (SLI) batteries became established. This trend was driven by concurrent requirements for maintenance-free operation (i.e., no watering and no acid mist) and for automated and continuous manufacture. The first commercial maintenance-free SLI batteries were made by the battery division of General Motors using expanded grid technology [1, 2]. One of the problems encountered with batteries containing expanded, or book-mould cast, PbCa grids was rapid loss of deep-discharge capacity with cycling. This

*Author to whom correspondence should be addressed.

0378-7753/91/$3.50

high rate of capacity loss, more severe than observed for batteries made with comparable lead–antimony alloys, has come to be called the 'antimony-free effect' [3, 4]. The rapid capacity loss associated with antimony-free grids was attributed to the absence in the grid of antimony that controls PbO_2 crystal morphology [5, 6]. These conclusions were, however, based on comparisons between grid alloys containing high antimony levels and antimony-free grids, which were also tin-free.

In later work [7], it was found that rapid failure of lead–calcium alloy cells could be induced by a so-called '23:1' shallow cycling routine. Following a 1-h discharge at the $C/10$ rate, the cells were charged at constant current until they reached 2.35 V/cell, where they were held for the balance of the 23-h charge. This regime was similar to one used by Naval Applied Science Laboratory workers [8] and others, to simulate battery duty cycles that sometimes caused severe premature positive-plate polarization and cell failure for thin-plate PbCa cells in submarine service. It was found that, under these conditions, a rectifying film developed between the positive grid and the active material and tin was mentioned as a possible preventive alloying agent [7]. The Naval researchers [8], however, had attributed the problem to formation of an insulating $PbSO_4$ barrier layer on the grid. Later, the mechanism of passivation was referred to as a 'tin-free effect' [9].

There is still controversy about the roles played by the active material and the grid/corrosion-layer interface in the capacity loss mechanism. A comprehensive understanding does not yet exist, but the role of the interface is certainly regarded as important. Research on the corrosion resistance and interfacial properties of PbCa alloys has been carried out in a number of laboratories [8–17]. Major studies were done at Battelle Europe for a world-wide group of lead/acid battery companies. Although the results of these investigations are available only to the sponsors [18], discussions with researchers who carried out related studies have suggested the importance to capacity retention of several plate processing variables, such as those shown in Table 1.

Since few authoritative results have been published, especially for expanded grids, the present work was carried out to determine the effects of some of the above variables, and of charging and some other operating and fabrication conditions, on the cycle-life performance of plates made with expanded PbCa alloy grids.

TABLE 1

Variables affecting capacity retention

1. Alloy tin content	5. Curing conditions
2. Plate thickness	6. Forming acid and current
3. Paste pellet size	7. Paste density
4. Active material confinement	8. Paste/electrolyte additives

Experimental

Variables investigated

Sixty cell configurations (127 cells) were assembled and cycled, each at least in duplicate, incorporating variations of the following parameters:

- grid alloy (pure lead, lead–calcium with several tin levels, lead–antimony)
- grid type (expanded cast or wrought strip, reinforced expanded, book-mould)
- positive paste density (3.9–4.3 g cm^{-3})
- curing temperature (40 and 80–85 °C)
- paste additives (Sb, Co, Bi, Te)
- electrolyte additives and acid concentration or circulation

Effects of extent of recharge, electrolyte circulation, plate compression, depth-of-discharge (DOD), and open-circuit stand were also evaluated by comparisons of performance under varied conditions with that under the standard conditions described below.

Standard experimental cell configuration

All cells were constructed with three negative and two positive plates. The positive-plate capacities were approximately 12.5 A h/per cell at the *C*/5 rate. This was about 45% of theoretical capacity. The capacity was higher (~50%) for low paste densities and lower (~35%) with phosphoric acid additives. All of the plates were enveloped in Daramic® separators. The positives were also wrapped with one layer of a glass-fibre matting. The five battery plates of each cell were sandwiched between two 3-mm thick PVC backing plates and the assembly was held together by six PVC nuts and bolts located at the top corners and centre edges of the backing plates. The bolts were tightened as consistently as possible in order to provide slight, but equal, pressure on the battery plates in all the test cells. Each assembly was then placed in a compartment of a commercial three-cell plastic battery case. This arrangement provided a slight excess of electrolyte volume in comparison with conventional batteries, due to the 'dead space' created by the nuts and bolt heads protruding beyond the plane of the backing plates.

All grid dimensions were 2 in. × 4 in. (5 cm × 10 cm). Expanded grids were made from 0.050–0.055 in. (1.3 mm) thick, continuously cast, or wrought, strip. Book-mould grids were cut to size from full-size golf-cart grids. The vertical members of the book-mould grids were 0.09 in. (2.3 mm) thick and approximately circular in cross section, while the horizontal members were 0.063 in. (1.6 mm) thick and of triangular cross section. Borders were 0.105 in. (2.7 mm) thick, but only the top and one side border were left on the experimental grid after trimming to size.

As far as possible, all of the plates were pasted to the same thickness (approximately 0.13 in. (3.3 mm)) with about 65 g of paste made from a Barton pot leady oxide. All of the negative plates were prepared with expanded cast lead–calcium–tin (PbCaSn) alloy grids. Initially, Pb–

0.06wt.%Ca–9.3wt.%Sn (603) was used but, in later work, Pb–0.09wt.%Ca–0.4wt.%Sn (904) was employed for negative grids. The paste contained an industrial battery expander (National Lead KX) and synthetic fibres, in addition to the leady oxide and sulphuric acid. The positive plates also contained synthetic fibres (equal quantities of $\frac{1}{4}$ and $\frac{1}{8}$ in. (6 and 3 mm) length material). The leady oxide and sulphuric acid ratios were adjusted to provide the desired wet-paste density.

The standard curing conditions, used for all of the negative plates and most of the positive plates were 80 or 85 °C and 100% relative humidity (r.h.) for at least 5 h. As a variation, some positive plates were cured at 40 °C and 100% relative humidity for at least 24 h, followed by several hours at a lower (80%) relative humidity.

Formation was carried out in 1.10 sp.gr. H_2SO_4 at 5 mA per cm^2 of positive-plate surface area for 55 h to provide approximately 200% of the theoretical charge. After formation, the forming acid was removed and replaced with the standard H_2SO_4 solution of 1.25 sp.gr. or other electrolytes of interest. Cells were then charged at 1.0 A until cell voltages remained relatively constant with time. About five charge/discharge cycles were carried out to determine the Peukert characteristics and nominal cell capacities, in particular, at the $C/5$ discharge rate for later cycling. The standard positive-plate active material, to which all variations were compared, was made with a wet-paste density of 4.25 g cm^{-3} and had a utilization of about 0.10 A h g^{-1}, about 45% of theoretical capacity, or about 12.5 A h/cell.

In order to keep track of changes made from one stage of the work to another, the stages are referred to as Series I, Series II, Series III, or Series IV.

Cycling and standard cycle regime

Following the Peukert characterization, cycling was carried out at the nominal $C/5$ discharge rate (2.5 or 2.75 A) to a 1.75 V cut-off, i.e., 100% nominal depth-of-discharge. Cells that reached the 1.75 V cut-off before 5.5 h of discharge were left on open-circuit for a minimum of 15 min until the total elapsed time, from the beginning of discharge, was 5.75 h. The standard charging current (1.58 A) was selected so that 115% of the previous discharge was replaced within 10 h, or proportionately less if the previous discharge was less than 5.5 h. In later work (after Series II) this standard current was altered to 1.2 A for 12 h to return 105% of the previous discharge. A minimum 15 min rest period on open-circuit also followed each charge so that the total cycle time was 16 h (or, later, 18 h). At every 10th cycle, an equalizing charge was provided in which all of the cells were charged for the full 10 h regardless of the duration of the previous discharge. Cells were considered to have failed, and cycling was discontinued, when the duration of the discharge was less than 50% of the original capacity.

Both formation and cycling were carried out with the cell jars partially immersed in a water bath held at 40 °C. Water additions were regularly made to the bottom of the cells, by injection of water through a partially immersed

glass tube, to make up for losses due to gassing and evaporation. The additions were made at the end of discharge, when the cell acid's specific gravity would be at a minimum, to allow the gassing during the subsequent charge cycle to mix the added water with the acid prior to the next discharge. Periodically (and for part of the study, continuously) the potentials of both positive and negative plates were measured relative to a reference electrode to ensure that the discharge capacity was limited by positive plate polarization and to monitor the range of positive-plate potentials. The end-of-charge positive-plate potential was typically 1.39–1.45 V with respect to a $Hg/Hg_2SO_4/1.25$ (or 1.27) sp.gr. H_2SO_4 reference electrode, and the negative plate potential was −1.4 to −1.5 V. (The potentials were smaller after cycling of cells with metal oxide additives or antimonial grids.) Cell voltages at end-of-charge were 2.7 to 2.85 V (or as high as 2.90 V during the extended overcharge). At cycle No. 80, for Series I cells, cycling was interrupted after fully charging and one positive plate from one cell of each type was removed for examination. Plates removed from test cells were first thoroughly rinsed in running water to remove acid and then dried in an oven at 60 °C. Grid growths were determined by comparing contact X-radiographs of the plates taken before forming and after removal from test. As cycling was continued beyond 80 cycles, cells were removed upon failure. After 150 cycles, the second positive plate was removed from the same cell as that from which a plate had been removed at 80 cycles. The remaining cells continued to cycle with two positive plates until failure (less than 2.5 A h discharge capacity). By contrast, for Series II–IV cells, the positive plate removals were made at 30 and 80 cycles. Since the cycling equipment was only capable of controlling 36 cells at a time, and because changes were made in response to on-going experimental findings, the work was carried out in several stages.

Variables investigated

The first stage of the investigation was divided into two parts. Initially 36 cells (18 cells in duplicate) were formed and cycled as a group (Series I cells). Then, an additional 12 cells (6 duplicates) were prepared and cycled (Series Ib). For all 48 cells, the overcharge factor was 115% of the previous discharge and the plates were tightly compressed, as described earlier. The electrolyte was the standard 1.25 sp.gr. H_2SO_4 although, for four cells in Series Ib, 1.8 wt.% phosphoric acid was added. Other parameters that were varied included grid type and alloy, curing temperature, and paste density. The variations are shown for these cells in Table 2, which also gives grid types and alloy codes. The CX prefix indicates an expanded, cast-strip grid. RX is an expanded, wrought-strip grid and BM is a book-mould, cast grid. Alloy designations are given as 3 wt.% Sb for commercially supplied three-percent antimonial lead grids, and by a three or four digit code for other lead or lead–calcium–tin alloys. The last two digits of this code indicate the tin content in tenths of a percent by weight and the first digit(s) indicates the calcium content in hundredths of a percent. One positive and one negative

TABLE 2

Variables investigated, Series 1 cells

Grid type and alloy	Wet paste density ($g\ cm^{-3}$)	Curing temperature (°C)	Electrolyte 1.25 sp.gr. plus
CX:000, 300, 303, 310, 600, 601 CX: 603, 603[a], 609, 1004, 1007 RX: 707[a], 0.25wt.%Sb–0.25wt.%Sn RX: 2.5wt.%Sb–0.25wt.%Sn; BM: 3wt.%Sb	4.25	80	
CX: 603; BM: 1105, 3 wt.% Sb	3.90	80	
CX: 603; BM: 3 wt.% Sb	4.25	40	
CX: 600[a], 1004[a]	4.25	80	1.8 wt.% H_3PO_4

[a] Series Ib cells.

TABLE 3

Variables Investigated, Series 2 cells

Grid type and alloy	Wet paste density ($g\ cm^{-3}$)	Curing temperature (°C)	Electrolyte sp.gr.	Overcharge factor (%)
CX: 600, CX: 603 (loose)	4.20	40	1.25	105
CX: 600, 603	4.20	40	1.32	115
CX: 603	4.26	85	1.25	115
CX: 603	4.20	40	1.25	115

plate was removed from one of the cells for examination at 80 cycles and the remaining plates were removed from the same cell at 150 cycles.

In order to obtain further information on the effects of acid concentration, curing and overcharge, a second series of cells (Series II, Table 3) was assembled with Pb–0.06wt.%Ca grids, with and without 0.3 wt.% Sn, and cycled as before. One pair of these cells contained plates with 603 grids that were not compressed between backing plates, so that there was very little pressure exerted on them by adjacent plates. Plates were removed from one of the cells for examination at 30 and at 80 cycles.

In an effort to reduce the importance of grid corrosion as a failure mode, as later discussed, a further series of cells (Series III, Table 4) was assembled for cycling with less overcharge and at a lower charging current. The cycle regime was altered to return 105% of the previous discharge at 1.2 A over a longer period of time (12 h). In an effort to reduce the effects of grid growth, higher-calcium alloys were used and some variations of grid geometry were investigated: incorporation of rigid side members (soldered Pb–1wt.%Sn strips) on expanded grids; and of book-mould grids with thinner

TABLE 4

Variables investigated, Series 3 cells

Grid type and alloy	Electrolyte sp.gr.	Paste additives	Other variations
CX: 000, 606, 900, 901, 903 RX: 2.6wt.%Sb–0.35wt.%Sn BM: 1005, 3wt.%Sb–0.41wt.%Sn	1.25		
CX: 000, 900, 903	1.32		
CX: 903	1.25		Acid circulation
CX: 000, 903 (frame)	1.25		Side-member
CX: 000, 800	1.25	0.1 at.% Sb_2O_3	
CX: 800	1.25	0.1 at.% Bi_2O_3	
CX: 800	1.25	0.1 at.% Co_2O_3	115% Recharge
CX: 800	1.25	0.1 at.% TeO_2	after cycle 30, except 10X cycle

wires (cross sections of 1.3 × 1.1 mm and 1.3 × 0.8 mm, compared to the 2.3 and 1.6 mm thick wires, respectively, in grids used previously), to make them more comparable with the thin expanded grids. The compositions of these book-mould grids were Pb–0.1wt.%Ca–0.5wt.%Sn and Pb–3.0wt.%Sb–0.4wt.%Sn. All negative grids were expanded Pb–0.09wt.%Ca–0.4wt.%Sn cast strip. In this series, the effects of tin additions, as well as of various metal oxide paste additives, were also examined.

A final series of cells (Series IV, Table 5) was assembled, this time with some cells in triplicate, to confirm and extend the previous findings and to permit duplicate cells to cycle to failure after removal of plates from one cell at 30 and 80 cycles. All of the cells in the top half of Table 5, above the 80%

TABLE 5

Variables investigated, Series 4 cells

Grid type and alloy	Curing temperature (°C)	Electrolyte sp.gr.	Paste additives	Overcharge factor (%)	Other variations
CX: 903	85	1.15		105	
CX: 609, 800, 903 CX: 0.23 wt.% Sb CX: 903 (frame)	85	1.25		105	
CX: 903	85	1.35		105	
CX: 800	40	1.25		105	
CX: 903	85	1.25		105	80% DOD
CX: 903	85	1.25		105	OC Stand
CX: 000	85	1.25	1.0 at.% Sb_2O_3	105	
CX: 000	85	1.25	1.0 at.% Bi_2O_3	105	
CX: 000	85	1.25	1.0 at.% Co_2O_3	115	
CX: 000	85	1.25	1.0 at.% TeO_2	115	

DOD entry, except for the 609 grids, were tested in triplicate; the rest were tested in duplicate. In this set, paste additives at higher levels than before, electrolyte sp.gr. and grid-alloy Sn were studied. Two cells were left on open-circuit for 120 days at 40 °C after charging and two cells were cycled to only 80% DOD.

Results

Figure 1 shows cycling results, under the 'standard' experimental conditions, for six individual cells, two with 601 grid alloy and four with 603 alloy. The 601 and the 603 Series 1 cells were cycled simultaneously, while cycling for the 603 Series 2 cells was initiated approximately four months later. Sharp increases in capacity at cycle 13 or 10 (Series 1 or Series 2, respectively) were due to replacement of the electrolyte with fresh acid. Removal of one positive and one negative plate from the first cell of each pair at 80 cycles, followed by an overcharge of all cells, sometimes resulted in a large change of capacity at cycle 80. For some cells, cycling was terminated at cycle 80 because of breakage of the remaining positive grid of the disassembled cell, due to handling and/or corrosion. If the remaining variability of capacity is assumed to be due to uncontrolled random differences among cell variables, a standard deviation of about 2% of theoretical capacity (5% of absolute capacity) may be taken as a measure of the reproducibility of the

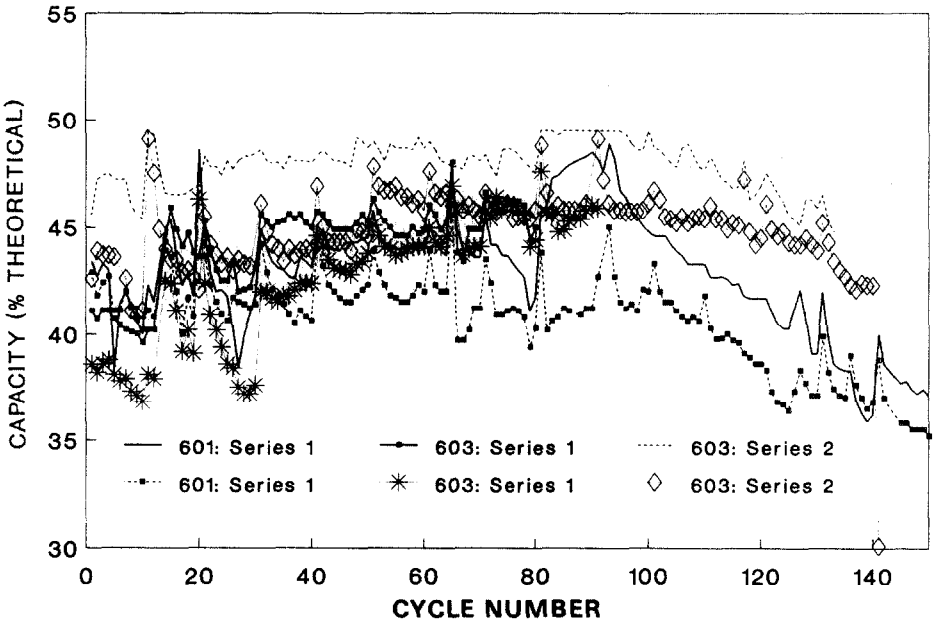

Fig. 1. Deep-discharge performance of six individual cells, containing 601 and 603 alloy grids, cycled at different times (Series 1 and 2) with 115% recharge.

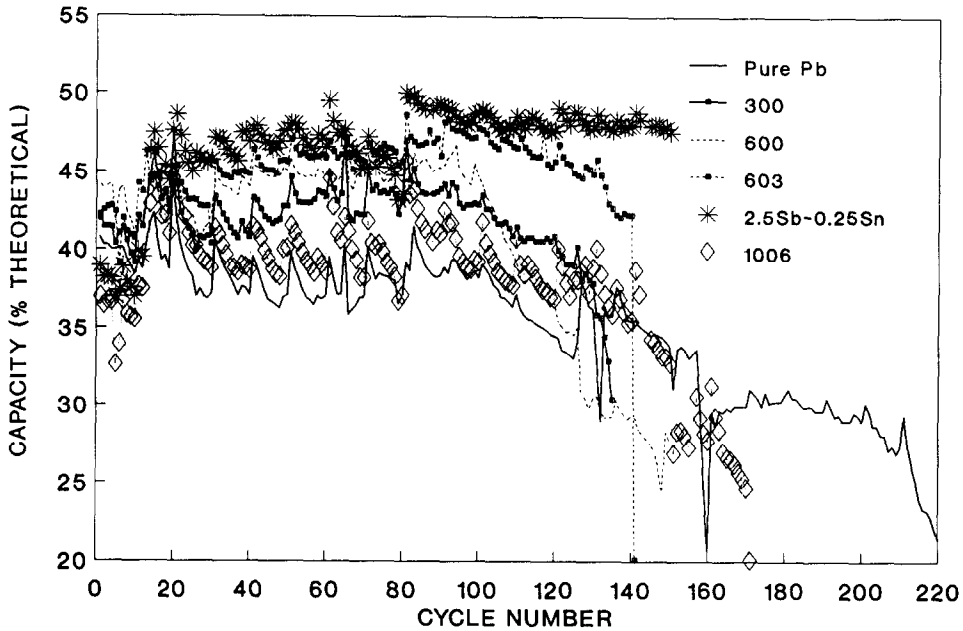

Fig. 2. Deep-discharge performance with 115% recharge for cells containing various grid alloys: averages of two cells for each alloy.

results. Thus, differences between cells smaller than 2% of theoretical capacity will not be considered significant.

The general pattern of cycling observed with this degree of overcharge (115%) was a small decline in capacity, followed by complete recovery with the more extended overcharge every 10th cycle. Some variations in this pattern occurred, primarily as a result of water additions. The dischargeable capacity remained constant, apart from changes due to such identifiable causes, until about cycle 100 for the plates of Fig. 1. After cycle 100, a roughly linear loss of capacity was observed, associated with corrosion of the relatively thin grids and possible other effects, as discussed later. In Fig. 2, as in later Figures, the average capacities for at least two cells, rather than those of individual cells, are shown. A gradual loss of capacity, only after extended cycling, is seen clearly for a number of non-antimonial grid alloys. The lead–antimony alloy showed an arrest in its previously increasing capacity. Vertical grid growth was 8–10% (area growth ~20%) at 80 cycles, with a small further increase with cycling. There was a strong dependence of growth rate on acid concentration and a much slower growth at the lowest acid gravity [19] but, except for a somewhat larger growth for high-Sn alloys, there was no significant dependence on grid alloy. Grid growth was, however, slightly less for plates with low-density paste, and was substantially less for the thicker book-mould grids than for the thinner expanded ones [19]. Reinforcing side-members on expanded 903 grids reduced grid growth and

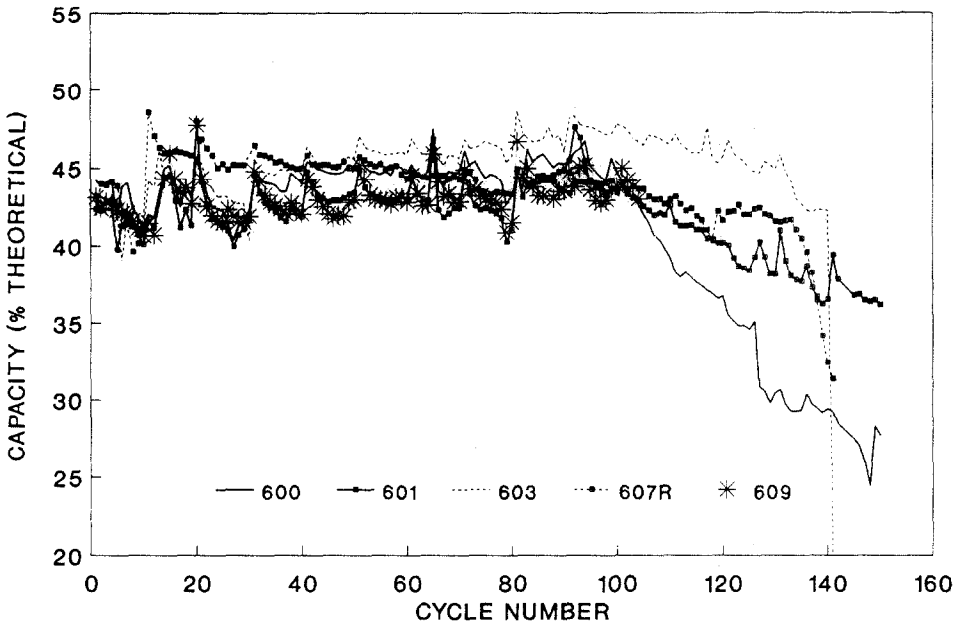

Fig. 3. Deep-discharge performance with 115% recharge for cells containing Pb–0.06wt.%Ca grids with various tin levels: averages of two cells for each alloy.

extended cycle-life. With pure Pb grids, the rigid frames had little effect on capacity retention although they did reduce grid growth. Grid growth at 80 cycles appeared to correlate well with cycle-life. If growth was a critical failure-inducing mechanism, then the choice of a grid alloy with high creep strength and low corrosion rate would be beneficial to lifetime. Results of this work were inconclusive, and are not presented here, although they suggested that the 603 alloy with 105% recharge was superior to 903 in capacity retention. From the results shown in Fig. 3, no effects due to the addition of tin can be discerned, except possibly after 100 cycles during the period of declining capacity. The addition of tin to Pb–0.03wt.%Ca alloys (not shown), also apparently had no significant effect on capacity for the first 100 cycles.

Only for the first 20 cycles did plates made with low-density pastes, or cured at the low temperature (40 °C), show significantly higher capacity than the plate processed through the standard conditions for expanded-cast Pb–0.06wt.%Ca–0.3wt.%Sn grids. For both of these variations in plate processing conditions, however, the capacity began to fall after about 80 cycles. These cycling curves are not shown, but both the plates cured at low temperature and those made with low-density paste behaved almost identically, after 80 cycles, to those shown for the 600 alloy in Fig. 3. The book-mould Pb–3.0wt.%Sb grids (Fig. 4), which were much thicker than the expanded grids, gave correspondingly longer cycle-lives. Under standard

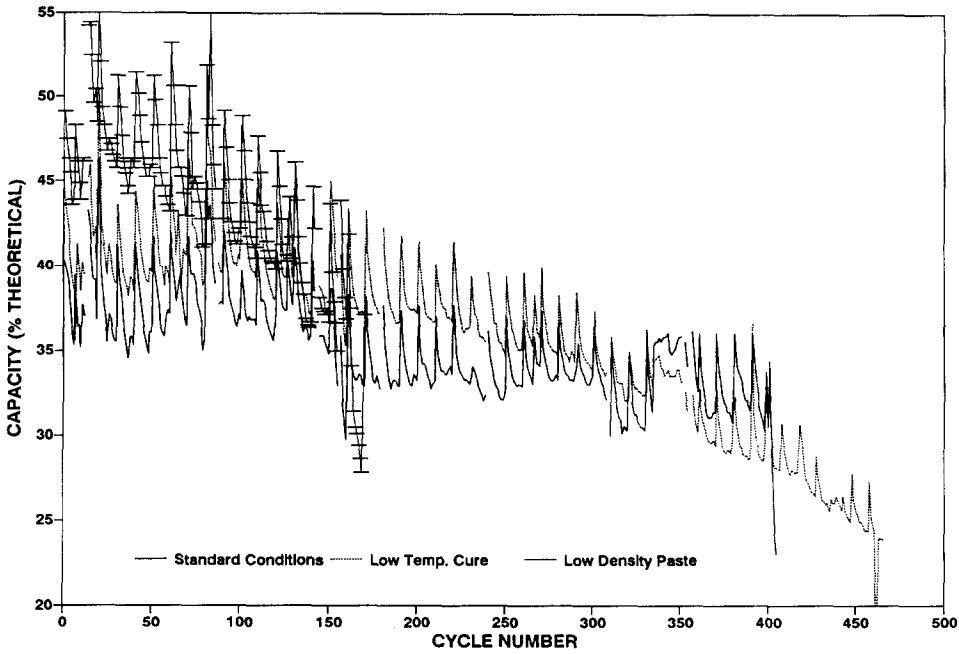

Fig. 4. Average deep-discharge performance with 105% recharge for cells containing Pb–3.0wt.%Sb grids for various paste processing conditions.

conditions, there was little change in capacity between 150 and 400 cycles, prior to a sudden drop just after 400 cycles. The plates cured at low temperature (40 °C) showed a gradual loss of capacity from 150 cycles until the failure criterion was reached at 450 cycles. The capacity was only slightly higher than that cured under standard conditions during the first half of its cycle-life. Plates made with a low-density paste had substantially higher capacities for well over 100 cycles, but failure occurred much sooner and more abruptly. Although active material variables, such as paste density, appeared to have some effect on initial capacities and capacity retention on cycling, there was no effect of grid composition variables on initial capacity. Antimony-containing grids at first showed some increase in capacity with cycling (Fig. 2). After this, there was little change in discharge capacity, and no effect of Sn content, for the first 100 cycles (Fig. 3). These findings were somewhat surprising, in view of the hypotheses being tested, that Sn was important to capacity retention in non-antimonial cells.

The effects of extent of recharge and plate compression, as well as Sn content, are shown in Fig. 5. For the 603 alloy, no loss of capacity for the first 80 cycles can be seen with 115% charge returned. When only 105% of the charge was returned, however, a steady decline of capacity occurred. Although part of this capacity was recovered with the overcharge each 10th cycle, some was irreversibly lost. The rate of capacity loss was very similar

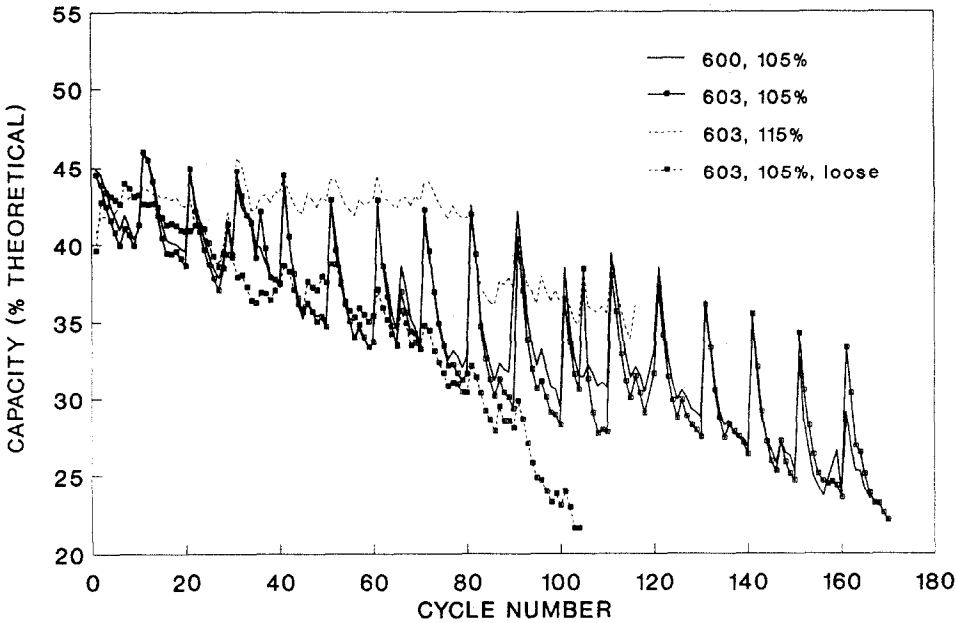

Fig. 5. Average deep-discharge performance with 105% or 115% recharge for cells with 600 and 603 grids, tight-packed and loose; 40 °C curing temperature.

for a loosely supported plate with 105% charge returned. Nevertheless, the capacity recovered every tenth overcharge was less and the rate of degradation of capacity accelerated after about 80 cycles. For the well-supported plates, the rate of capacity lost was almost identical, with or without 0.3 wt.% Sn, in the Pb–0.06wt.%Ca grid alloy. There was also no difference between the behaviour of the 600 and 603 alloy with 115% recharge (Fig. 6) in a more concentrated electrolyte (1.32 sp.gr.). Although the grid alloy had no effect, the initial capacities were higher and decreased more rapidly in the more concentrated acid. The absence of any significant effect of grid alloy composition for non-antimonial alloys, even with only 105% recharge, can clearly be seen in Fig. 7. Accordingly, the data for all the non-antimonial plates cycled in 1.25 sp.gr. acid were combined in order to make comparisons at a higher acid gravity, with wrought antimonial and calcium grids, and with plates made with active material additives. Initially, plate performance with 1.32 sp.gr. acid was similar to that with 1.25 sp.gr. but the rate of loss of capacity was somewhat greater at the higher acid gravity (Fig. 8). No differences were observed between expanded wrought and expanded cast PbCaSn strip grids (Fig. 9). By contrast, expanded wrought Pb–2.6wt.%Sb–0.4wt.%Sn grids failed rapidly, within 20 to 40 cycles. When the cells were disassembled, the top bars of all grids had broken or the grid wires had separated from the top bar.

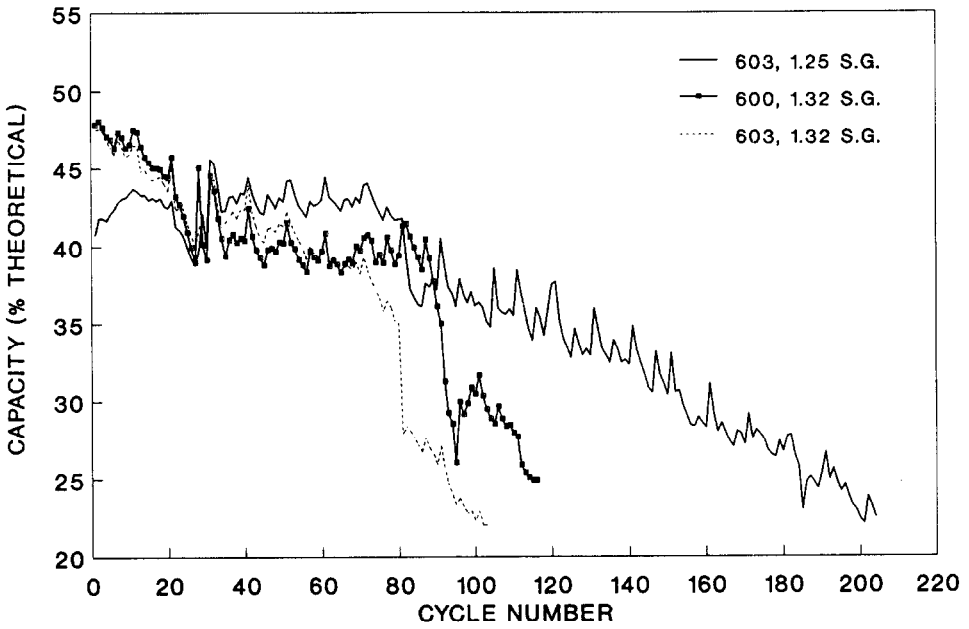

Fig. 6. Average deep-discharge performance with 115% recharge for cells with standard and high acid concentrations, 40 °C curing temperature.

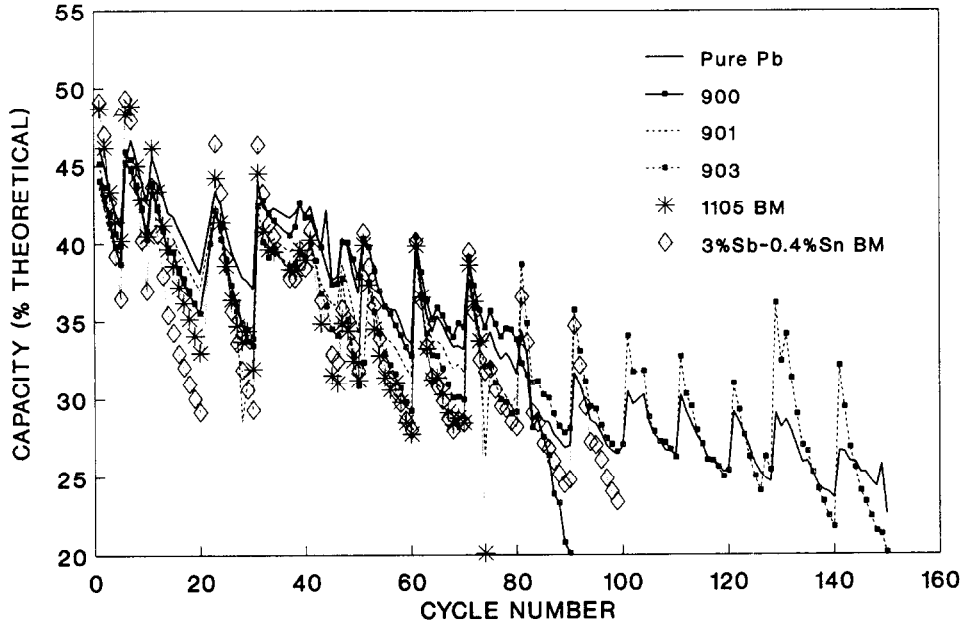

Fig. 7. Average deep-discharge performance with 105% recharge for various grid alloys.

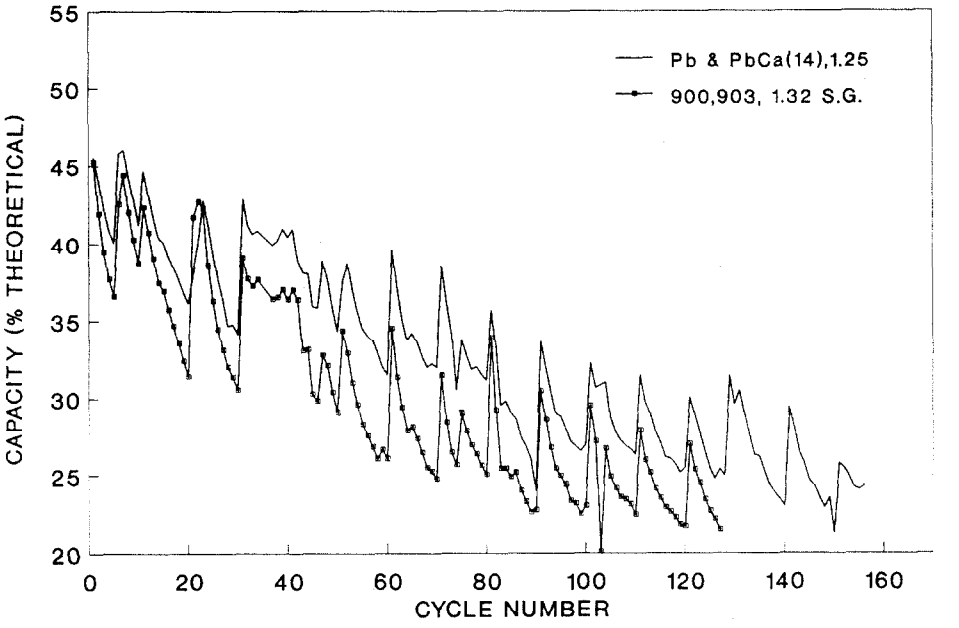

Fig. 8. Effect of acid concentration with 105% recharge for non-antimonial grid alloys: cell averages.

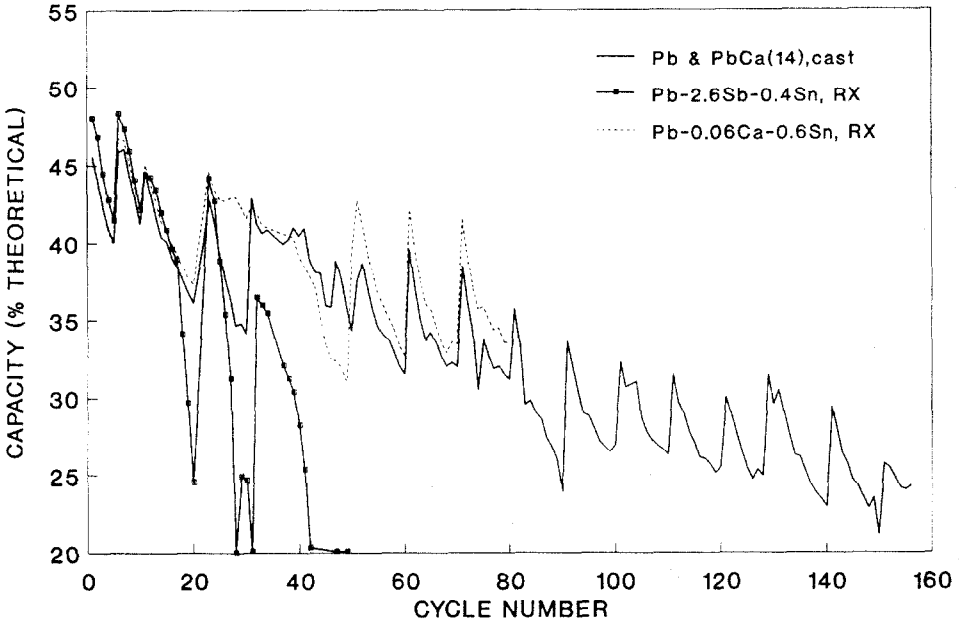

Fig. 9. Effect of grid alloy on cycling performance with 105% recharge: cell averages.

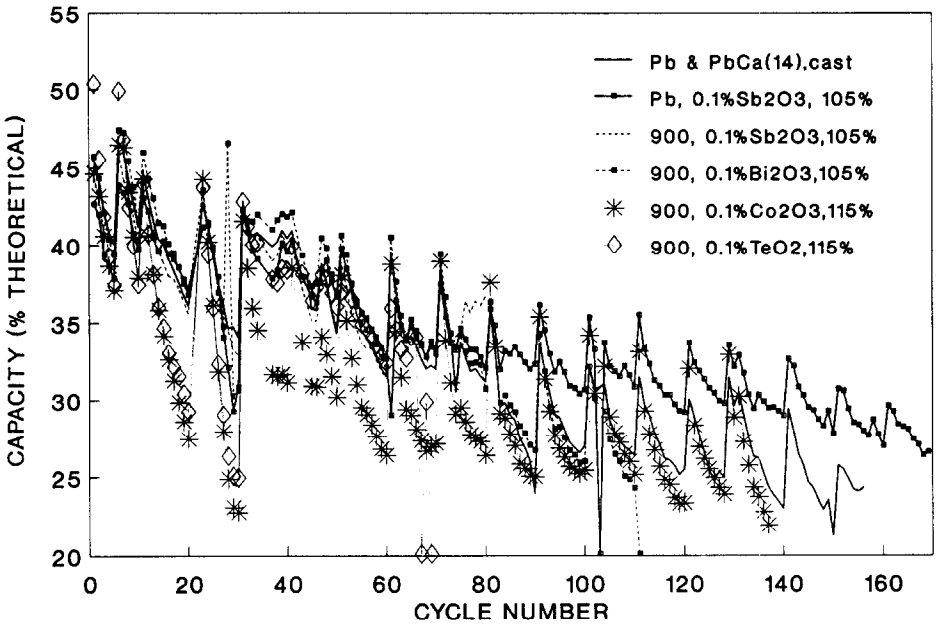

Fig. 10. Effect of metal oxide additives on cycling performance with 105% (or 115%) recharge: cell averages.

When 0.1 at.% of Bi_2O_3 and Sb_2O_3 were added to the active material of Pb or Pb–0.09wt.%Ca expanded grids (Fig. 10), there was no significant effect on capacities or rate of capacity loss until after cycle 80. For the pure Pb grids, improved capacity retention was found due to additions of Sb_2O_3 and Co_2O_3. (It should be noted that the data for pure Pb grids with 0.1 at.% Sb_2O_3 addition is for one cell only, since anomalously high capacities were obtained for the other cell following the routine plate removal at thirty cycles.) However, the extent of overcharge had to be increased from 105% to 115% to maintain the rates of capacity loss in the cells with Co_2O_3 and TeO_2 additives, which did not appear to be adequately recharged at 105%. Even at 115%, there were indications that the plates with Co_2O_3 were not sufficiently charged, except during the extended overcharge every 10th cycle when the capacities exceeded the average of the 14-cell control group. Similar results were obtained with the additions of 1.0 at.% of these additives, except that the capacities of the Co_2O_3-containing plates fell below those of the control cells, apparently due to inefficient recharge and, possibly, self-discharge. Capacities of plates with 1 at.% Sb_2O_3 and pure Pb grids slightly exceeded those of the controls after cycle 100. The effect of electrolyte density, in comparison to the 1.25 sp.gr. acid, was to give a low capacity at low acid gravity and little change with cycling, and about the same capacity initially with a high-acid gravity, but a more rapid failure of the plate, as shown in Fig. 11. The rapid failure was caused by shorting induced by excessive grid

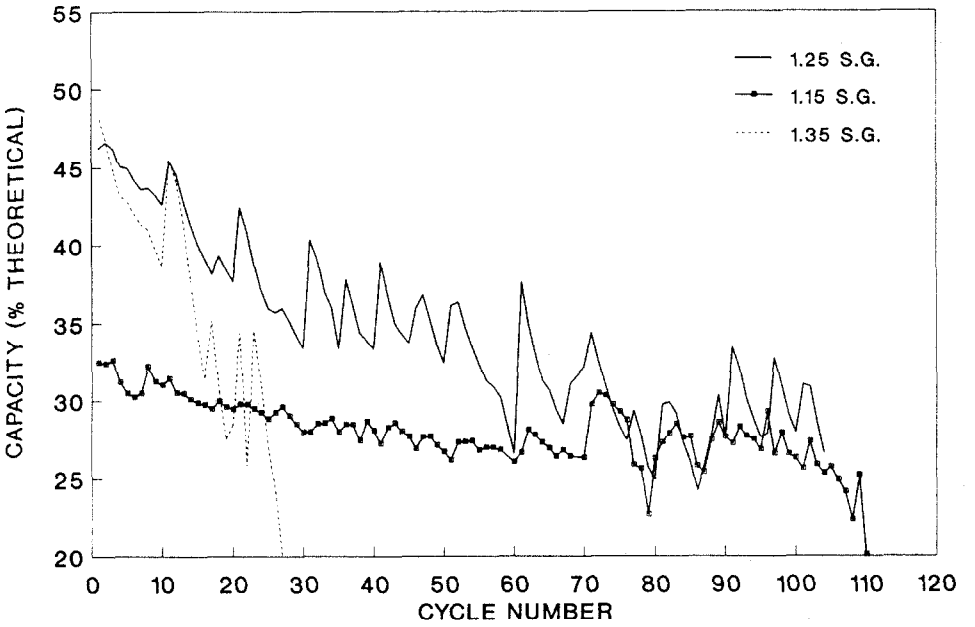

Fig. 11. Effect of electrolyte concentration on capacity with 105% recharge for 903 grids: cell averages.

growth. For 115% recharge (Fig. 6), a higher initial capacity was obtained at 1.32 sp.gr. The smaller effect of acid concentration at 105% recharge may have been due to the competition between opposing effects of poorer recharge efficiency and greater discharge depth (due to better acid availability) at higher acid concentrations. Low initial and slowly decreasing capacities were, however, observed with 1.15 sp.gr. acid. Phosphoric acid additions (with 115% recharge) gave a low capacity, initially similar to that observed with 1.15 sp.gr. acid (Fig. 11). With phosphoric acid, however, the capacity slowly increased to approximately 36%, then slowly decreased, but remained above 30% for over 200 cycles. Although higher capacities, attributed to reduction of shedding, have been found for Planté plates, reduced capacities and extended cycle-lives for pasted plates have also been reported by several other workers [20, 21]. The optimum level of H_3PO_4 is somewhat lower than the 1.8% (22.5 g l^{-1}) used here; it depends on a number of parameters and, as has been suggested, should be referred to the amount of PbO_2 in the cell [21].

Further results and discussion

While the alloy composition appeared to have little effect on the rate of capacity loss during the first 100 cycles, it did affect cycle-life and the loss of capacity after 100 cycles. A much earlier consequence of Sn additions on

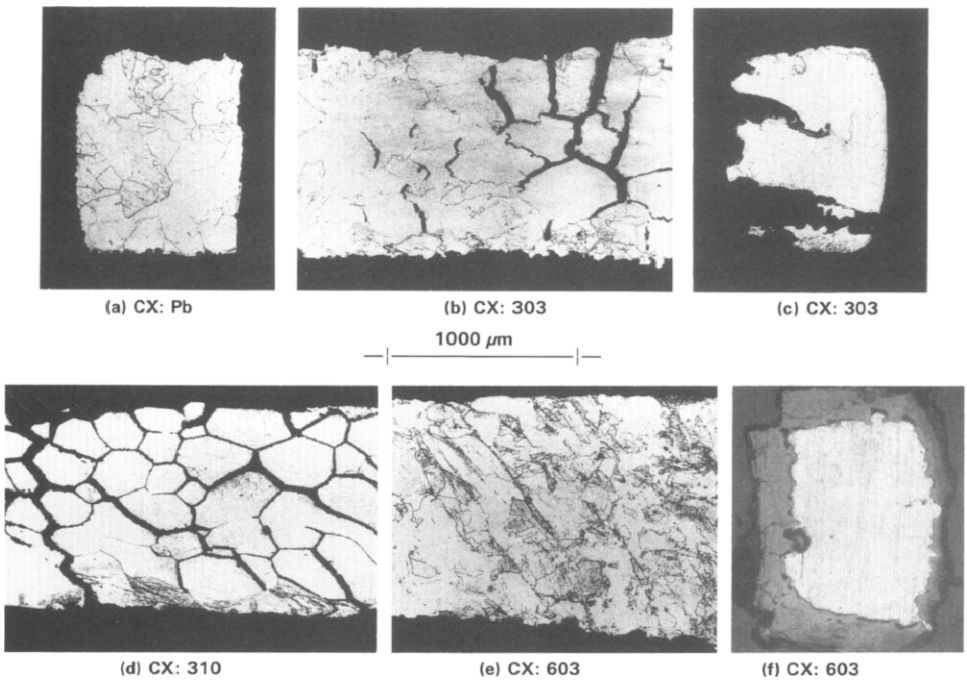

Fig. 12. Sections of grid wires after 80 cycles at 115% recharge: in 1.25 sp.gr. acid.

PbCa grid alloys had been expected as a result of influences on the structure of the interface between the grid and active material. With 115% recharge, the cycle-life turned out to be closely related to the corrosion characteristics and durability of the (relatively thin) grids and consequent effects on plate performance. Metallographic results of examination of grids after 80 cycles with 115% recharge are shown in Fig. 12.

For the metallography shown, the grids were first chemically stripped with alkaline hydrazine–dihydrochloride–mannitol solution, mounted in polyester resin and, after grinding and polishing, etched to reveal the microstructures with a citric acid–ammonium molybdate solution. This was preceded, in the case of lead–calcium alloys, by a brief chemical polish in acetic acid–hydrogen peroxide solution. Figure 12(a) shows a transverse cross section of a pure lead grid wire, indicating varying uniform surface corrosion consisting of shallow hemispherical pits. The chemical stripping has removed the corrosion layer but the extent of corrosion after 80 cycles was very little. Although corrosion ultimately is believed to have contributed to the decline of capacity associated with a long cycle-life for the other cell containing a pure lead grid, the immediate cause of failure for this cell appeared to be development of an interplate short-circuit.

Figures 12(b) and (c) show longitudinally sectioned and transverse sections of wires after the same cycle duration from a Pb–0.03wt.%Ca–0.3wt.%Sn (303) grid. Severe and penetrating corrosion has occurred selec-

tively along grain boundaries, particularly in regions of the grid where large straight-edged grains existed. The preferential attack was even more pronounced and dramatic in the longitudinal section of a Pb–0.03wt.%Ca–1.0wt.%Sn (310) grid wire shown in Fig. 12(d). As has previously been discussed [22], alloys that have an irregular grain structure are resistant to stress corrosion fracture mechanisms. If corrosion was uniform, capacity loss occurred gradually. Perhaps, sufficient metal loss had to occur before limiting the performance of the plate, although it is probable that other capacity reducing mechanisms were also contributing. If corrosion was penetrating, very rapid failures occurred, sometimes precipitated by cell disassembly for plate removal at 80 cycles. Since high tin:calcium ratios and low calcium levels promote the formation of a large-grained regular structure, with straight grain boundaries, along which fractures can propagate, dramatic examples of this corrosion mode could be seen in the low-calcium, high-tin grid alloys. At a higher (0.06 wt.%) calcium level with low (0.3 wt.%) tin, grain boundaries were much more irregular so that more uniform corrosion (Fig. 12(e)) was observed. A transverse cross section of an unstripped grid wire with a 200 μm thick intact corrosion layer is seen in Fig. 12(f). Approximately one-quarter of the initial metal had corroded at 80 cycles. Further sections of unstripped 603 grids are shown in Fig. 13(a) after 204 cycles in 1.25 sp.gr. acid at 115% recharge and in Fig. 13(b) after 103 cycles in 1.32 sp.gr. acid. An unstripped 600 grid, after 116 cycles in 1.32 sp.gr. acid, is also shown (Fig. 13(c)) for comparison. For each of these grids, even that which had achieved 204 cycles before half of the initial plate capacity had been lost, the corrosion did not appear substantially greater than it had been

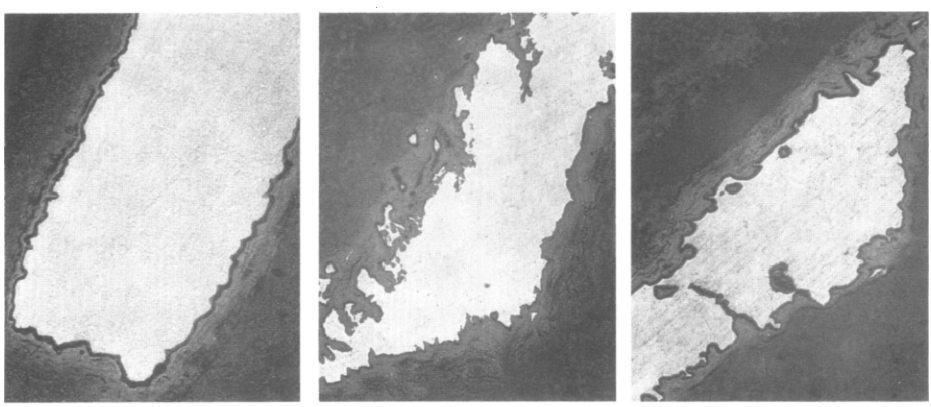

Fig. 13. Sections of expanded cast-strip grid wires and corrosion layers after cycling with 115% recharge in: (a) 1.25 sp.gr. acid, 204 cycles; (b) 1.32 sp.gr. acid, 103 cycles; (c) 1.32 sp.gr. acid, 116 cycles.

at 80 cycles. However, an inner compact duplex corrosion layer structure could be discerned clearly with polarized light microscopy. It consisted of a yellow–orange layer, 5–20 μm thick on the grid metal, overlain by a dense grey-brown layer, approximately 40 μm thick. Both of these layers can be seen, but with difficulty, in Fig. 13(a) where they appear as a very thin black zone on the light colored metal and a light-grey thin zone between that and the rest of the more porous corrosion product. Similar observations have been made for lead–calcium–tin and lead–low antimony plates left standing in low gravity acid [15] and for unsupported PbCaSn plates, cycled to rapid failure in 1.28 sp.gr., but not in low specific gravity acids [23]. It was found that the yellow–orange layer was rich in α-PbO.

A limited number of samples was extracted from the corrosion layers with a fine probe and submitted to X-ray diffractometry (XRD) in a special evacuated Debye Scherrer camera [24]. The presence of t-PbO in the yellow–orange layer was confirmed and the dark brown layer above it was identified as β-PbO_2 in a formed plate. In cycled plates, XRD of the corrosion layer revealed α- and β-PbO_2 but t-PbO was difficult to identify because of overlap between its diffraction lines and those of t-PbO_2. In this work, the dependence of initial utilization and of rate of capacity loss on acid concentration was similar to that seen in Fig. 11, if account is taken of the more porous active material (lower paste density) in the earlier study. This would have permitted a similar acid attack of the grid metal at lower acid concentrations than in the present work, which used higher and more conventional paste densities, even for the 'low-density' paste.

As the tin:calcium ratio was increased, deep penetrating attack occurred along particular straight boundaries, an extreme example of which is shown in Fig. 14(a). A further increase in calcium content had the effect of making the mode of corrosive attack much more uniform such as in the 904 alloy grid of Fig. 14(b), or the book-mould cast 1105 alloy grid in Fig. 14(c). Except for isolated cases, the attack of the Pb–3.0wt.%Sb alloy was very uniform (Fig. 14(d)), as was that on the expanded wrought strip Pb–2.5wt.%Sb–0.25wt.%Sn grid (Fig. 14(e)). This was also true for expanded wrought Pb–0.25wt.%Sb–0.25wt.%Sn (Fig. 14(f)).

It was found from the metallography of failed plates that there was more severe corrosion in grids from cells with more concentrated acid. This was in accord with the observations of higher rates of grid growth at higher acid concentrations [19] and shorter cycle-lives. For example, at 30 cycles, 903CX and 800CX grids had area growths of 14.2 and 11.2% in 1.25 sp.gr. acid and of 16.4 and 15.7%, respectively, in 1.32 sp.gr. acid. At least part of the growth appeared to be caused by expansion of the active material during discharge. If growth had been driven only by corrosion, it would have occurred at a uniform or accelerating rate during cycling. Instead, it occurred at a decreasing rate [19], so that most of the growth took place in the early cycles.

Higher rates of grid growth were also associated with higher tin contents for Pb–0.09wt.%Ca alloys. Lower rates of growth were found in

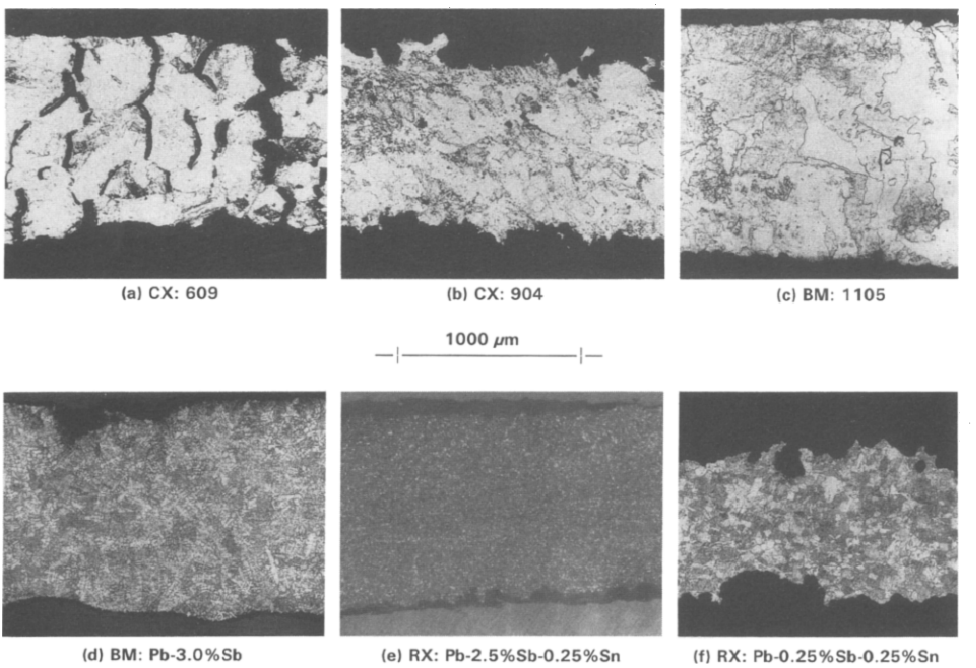

Fig. 14. Sections of grid wires after 80 cycles at 115% recharge: 1.25 sp.gr. acid.

1.15 sp.gr. acid and with Co_2O_3 and Bi_2O_3 additions in 1.25 sp.gr. acid, possibly due to positive plate depolarization in the case of Co_2O_3. Reinforcement of expanded grids with side members, or the use of thicker grid wires, also reduced growth and extended life. The dependence of growth on acid gravity for 903 grids has previously been reported (Fig. 6 in ref. 19 – note that the symbol for 1.32–1.35 sp.gr. acid in the caption to Fig. 6 should be ⊗, not o.).

It had been intended, as part of this work, to examine the corrosion layer and interface to determine whether divalent lead compounds, lead sulphate or lead oxides, were responsible for the sudden losses of capacity which had been observed in lead–calcium alloy batteries, long before grid corrosion became important. As discussed by Giess [9], at least two distinct and complex phenomena can cause such rapid losses of capacity. One (the antimony-free effect) is related to a kinetic hindrance of the electrochemical reduction of PbO_2 at low antimony concentrations (less than 2 wt.%). Even in the presence of up to 1.5 wt.% Sb in the grid alloy, however, poor charge acceptance caused by excessive positive plate polarizations occurred. The polarizations were related to corrosion of the current collector at low H_2SO_4 concentration, the formation of t-PbO and correspondingly increased ohmic resistance in the grid/active mass interface. This could be prevented by additions of 0.2–0.4 wt.% Sn and so this second mechanism, causing abnormal passivation with a poorly conducting lead species, was termed a 'tin-free

effect'. Giess showed that the addition of at least 0.2 wt.%–0.6 wt.% Sn to the grid alloy substantially reduced (short-term) grid corrosion and excessive polarization, not only for antimony-free (Pb, PbAs, PbCa), but also for antimonial, lead alloys (Pb–0.6wt.%Sb and Pb–1.5wt.%Sb–0.6wt.%As). For pure Pb, in the absence of Sn, the major component of the relatively thick (compared to Pb–0.6wt.%Sn) corrosion layer was found to be t-PbO, which formed underneath a 1–2 μm thick $PbSO_4$ layer. The mechanism of how Sn acts is not well understood. A strong effect of tin added to the electrolyte has also been reported for cells with (pure lead) Planté plates but could not be demonstrated for cells with pasted Fauré plates [25].

The passivation being considered is distinct from thermopassivation which occurs as a result of drying formed positive plates at temperatures above 70 °C. Thermopassivation is attributed to semiconductor properties of PbO_n in the corrosion layer [26] and has been found to be prevented by tin-plating of the grid [27, 28]. More needs to be learned about both thermopassivation and the phenomenon discussed here to determine what similarity there is between them.

Under the experimental conditions for the work described here, such a rapid loss of capacity occurred in none of the cells, except at the highest acid concentration (Fig. 11), whether they contained antimony or tin in the grid alloy, or not. Nakashima and Hattori [23] found no premature capacity losses when electrolyte concentration or quantity was restricted, but did so at high acid concentrations. They concluded that acid concentration during discharge was a critical factor. Much of their work, and that of Burbank [5, 6] was done with single positive plates, suspended in excess acid.

When a sudden loss of capacity occurred in this work, it was usually due to wire breakage and loss of grid integrity, caused by penetrating corrosion of unsuitable grid alloys. Capacity declines for the suitable alloys used (after Stage I) were gradual. Gradual thinning of grid wires or isolated breakages due to corrosion may have contributed to the decline, although the metallography of Fig. 13 and the similarity of the performances of the thicker book-mould grids and the thinner expanded grids (Fig. 7) suggests that it was not an important factor. Accumulation of a non-continuous barrier corrosion layer (see below) may also have contributed but, if so, it is hard to explain why high-antimony plates lost capacity at the same rate as the non-antimonial plates with 105% recharge (Fig. 7). Perhaps the capacity-loss mechanism for the antimonial plate was different (less efficient charging) than for the non-antimonial plates. Perhaps the capacity loss for non-antimonial plates was due to active material degradation or loss of electrical contact, or a combination of the above factors. Shedding was occasionally observed (e.g., for loosely retained plates recharged to 105%) but it was not usually pronounced. Sunu and Burrows [29] have suggested that conditions of insufficient overcharge cause stratification, producing non-uniform active material utilization and charging efficiency and, thereby, a capacity decline. Voss [30] found improved cycle-life with minimum overcharge for cells with acid circulation.

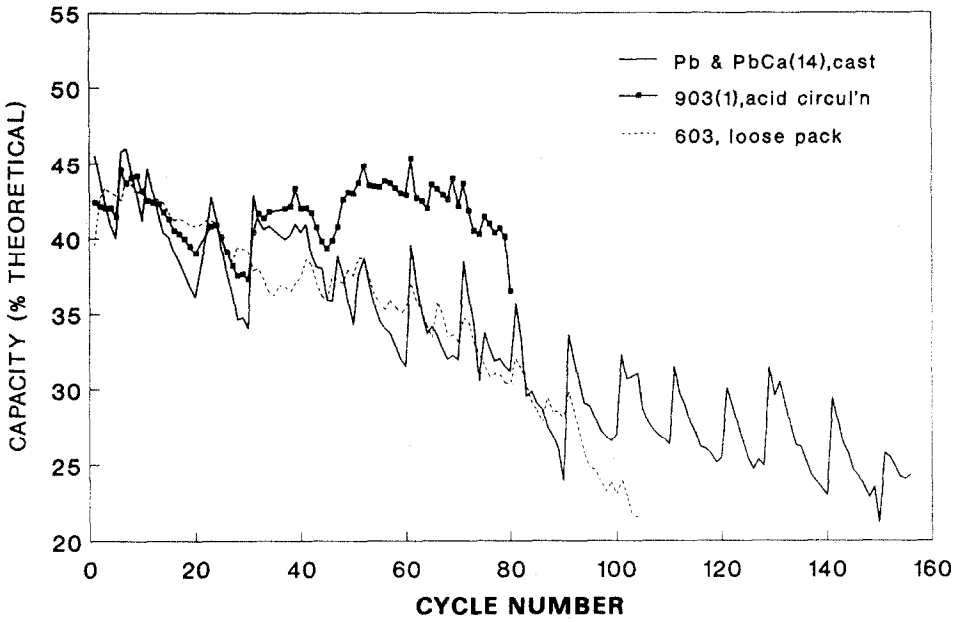

Fig. 15. Effects of acid concentration and stack compression in 1.25 sp.gr. acid with 105% recharge: cell averages. Curing temperature 40 °C for loose-pack 603 cell only.

Substantial stratifications were measured within these cells. In a typical case, with 105% recharge, the acid sp.gr. was 1.13 at the top of the cell and 1.30 at the bottom at the end of discharge, and the stratification was clearly reflected in non-uniform horizontal grid growth during cycling. The acid sp.gr. range was only 1.18 to 1.17 with acid circulation, and the capacity decline and the amplitude of the 10-cycle capacity waves were substantially reduced, as shown in Fig. 15. (The sudden drops in capacity at cycles 43, 51 and possibly 93, were associated with cracks in the cell case, possible leakage between acid and water bath, and probable reduction of cycle-life due to handling to correct these problems.) The wave amplitude could also be substantially reduced, indicating improved charging efficiency, by using a loose-fitting plate assembly, but the rate of capacity loss was then similar to that of a tight-packed cell without acid circulation, until a more rapid approach to failure after about 90 cycles (see also Fig. 5). More uniform corrosion and more complete utilization were obtained with circulation of 1.25 sp.gr. acid.

Although there was some indication of divalent lead compound formation between the grid and corrosion layer, obtained by polarized-light microscopic examination of samples mounted by vacuum impregnation with corrosion layers and active material intact, this was not associated with rapid failure, and was found even in freshly formed plates. In all but one experimental variation, plates were removed from the cell after a complete recharge. The only exception was for the cells left to stand on open-circuit

for 120 days following initial charge. Although an orange–yellow layer about 10 μm thick was observed between the grid and corrosion layer on a plate taken from this cell, the grid alloy contained 0.3 wt.% tin and the layer was not shown to be the cause of poor plate performance. In fact, such a layer was observed on a very large proportion of the well cycled non-antimonial grids examined, regardless of Ca or Sn content, and was even thicker on freshly formed grids. On the well cycled plates, it was not always continuous. It was visible on grids with 0.23 wt.% Sb but it was difficult to detect on the grids with 2.6 or 3.0 wt.% Sb or on a 903 grid which had only been discharged to 80% depth-of-discharge (154 cycles). All but the open-circuit-stand cells were charged before disassembly, and never experienced prolonged open-circuit stand in a partially discharged state. For these cells, it is likely that any interfacial barrier layers, which may have formed, were reoxidized during charge, even when recharge was limited to 105% of the previous discharge. In retrospect, more useful results may have been obtained if plates had been removed in a partially discharged state or if charging potentials had been limited to lower values. Since the work was carried out, there have been a number of informal or anecdotal reports of the observation of barrier layers of either lead sulphate or other compounds in batteries subjected to elevated temperatures and incomplete recharge. These conditions are very different from those in the experimental work just described. In some cases, researchers have attributed failures to an insulating $PbSO_4$ corrosion layer [8, 16, 31–33] or detected a layer of $PbSO_4$, without establishing whether it was continuous or affecting inhibiting electrode processes [34]. Development of the passivating $PbSO_4$ has been linked to the recharge conditions [8, 16]. In other work, performance losses were associated with the presence of a t-PbO layer on the grid [9, 10, 15, 20]. According to the models of Rüetschi [35] and Pavlov and Iordanov [36], a semi-permeable $PbSO_4$ layer must first be established in order to permit the formation of t-PbO. Thus, it is possible that various stages of the same process are being observed under different conditions. Alternatively, some conditions, such as porous or thin active materials or high acid gravities, may favour the formation of a rechargeable $PbSO_4$ on the grid surface, which is removed during charging, so that underlying t-PbO can only form during open-circuit stand. Still others [10, 37] have attributed the 'antimony-free effect' to differences in the nature and degree of cracking in the PbO_2 corrosion layers, related to stresses, and it was postulated that these were somehow relieved if their formation was influenced by antimony.

It is also possible that the lead sulphate, or t-PbO, or corrosion layer cracking is not the cause of the 'antimony-free' or 'tin-free' effect but a result of it. Winsel *et al.* [4] have argued that the reason for the effect is a changing current distribution from cycle to cycle, due to the changing conductivity of the PbO_2. They suggest that the so-called antimony-free effect would better be described as a 'relaxable insufficient mass utilization (RIMU)' because the phenomenon can occur both in the absence and the presence of antimony, and is due to solid-state relaxation processes in the non-stoichiometric PbO_2

electrode [38, 39]. They postulate that the RIMU is caused by an increasing electronic resistance within the active material, located in the narrow neck zones of the aggregate of spheres which make up the 'Kugelhaufen' PbO_2 electrode, which can be avoided by the choice of a suitable charging regime [4]. The charging regime specified [39, 40] for a Planté electrode consisted of a high initial current ($C/1$ to $C/2$ rate) for 65–70% charge returned, followed by limited overcharge (15–20%) at a lower current. An unfavorable charging regime said to cause rapid capacity decay was charging at a low rate ($C/10$) with excessive overcharge (50%). In this work, the $C/10$ charging rate was used without seeing a rapid capacity decay, although the extent of overcharge was limited within their prescription. They have also suggested that the effect of antimony may be to catalyze relaxation of the positive electrode towards the equilibrium state after charging [38], but the mechanism by which this may occur remains to be investigated.

The results showing effects of tin, in the grid alloys reported above, are applicable to battery applications in which corrosion, or corrosion-induced growth, is the predominant failure mode. In such applications, choice of appropriate grid alloy and sufficiently thick grids can be made to extend the cycle-life considerably. Further work is needed under different experimental conditions to explore the causes and remedies for rapid and sudden early battery failures. Such work is now being undertaken by D. A. J. Rand's group at CSIRO, Australia, with ILZRO support [41]. The laboratory reports on which this paper is based were made available to CSIRO at a special workshop organized to assist in planning the CSIRO project [42]. Some of the conclusions of this work and recommendations for further work are given below.

Conclusions and recommendations

1. A large amount of experimental work has been reviewed in order to reach conclusions about the experimental variables that affect the capacity degradation of non-antimonial grid alloys. The conclusions presented here are tentative. After a more thorough analysis of selected data, it may be possible to strengthen them further.

2. Under conditions whereby deeply cycled lead/acid plates containing lead, lead–calcium or lead–low-antimony grid alloys, are adequately recharged with minimal open-circuit stand in a discharged state, tin-free alloys do not necessarily suffer rapid or premature capacity loss and tin is not required in the positive plate grid alloy. Tin may have provided some benefit in reducing the rate of capacity loss in the late stages of cycling failure with 115% recharge, but no clear benefit was found with 105% recharge.

3. Under these conditions, long cycle-lives were obtained for pure lead grids, or for lead–calcium grids containing a low ratio of tin to calcium (less than about 5:1) and a moderately high level of calcium (at least 0.06 wt.%).

Such alloy compositions did not suffer penetrating corrosion or wire breakage, which could otherwise have caused early failures of the thin grids.

4. Capacity losses during cycling with limited recharge (105%) appeared to be due primarily to non-uniform, stratification-induced, active material degradation and/or loss of electrical contact, not to corrosion-layer passivation. Loss of electrical contact may have been related to isolation of active material and appeared to be related to grid growth, which was much more dependent on the rigidity or strength of the grid members than on alloy composition. Much higher grid-growth rates at higher acid concentrations were also associated with more rapid capacity-loss rates. Grid growth during early cycling appeared to be a useful predictor of cycle-life. This suggests that creep resistance, as well as corrosion resistance, should be considered when selecting grid alloys. The conclusions related to causes and effects of growth agree well with those reached by Enochs *et al.* [43], based on results with large motive power batteries, cycled to 80% DOD.

5. In further work, a cycling regime should be chosen to reliably produce corrosion-layer passivation in order to study its development and causes more exactly. Periods of open-circuit stand after discharge may be a critical component of such a regime. Interfacial examinations should be done of plates removed from cycling both in charged and in discharged states.

Acknowledgement

Helpful discussions about the experimental results and interpretation with Dr T. G. Chang are gratefully acknowledged.

References

1 E. G. Wheadon and N. L. Willmann, *U.S. Patent 3 881 952* (May 6, 1975).
2 E. Daniels, Jr. and R. H. Kline, *U.S. Patent 3 945 097* (Mar. 23, 1976).
3 J. Bohmann, U. Hullmeine, W. Kappus, E. Voss and A. Winsel, *ILZRO Project LE-277, Progress Rep. No. 8*, International Lead–Zinc Research Organization, Research Triangle Park, NC, Dec. 31, 1981.
4 A. Winsel, E. Voss and U. Hullmeine, *J. Power Sources, 30* (1990) 209.
5 E. J. Ritchie and J. Burbank, *J. Electrochem. Soc., 117* (1970) 299.
6 J. Burbank, *J. Electrochem. Soc., 111* (1964) 1112.
7 E. A. Willihnganz, personal communication, Aug. 15, 1978.
8 S. Tudor, A. Weisstuch and S. H. Davang, *Electrochem. Technol., 5* (1967) 21.
9 H. K. Giess, in K. R. Bullock and D. Pavlov (eds.), *Proc. Symp. Advances in Lead–Acid Batteries*, Vol. 84-14, Electrochemical Soc. Inc., Pennington, NJ, 1984, pp. 241–251.
10 K. Fuchida, K. Okada, S. Hattori, M. Kono, M. Yamane, T. Takayama, J. Yamishita and Y. Nakayama, *ILZRO Project LE-276, Final Rep. (Progress Rep. No. 8)*, International Lead–Zinc Research Organization, Research Triangle Park, NC, Mar. 31, 1982.
11 A. Arlanch, G. Clerici and M. Maja, in J. Thompson (ed.), *Power Sources 8*, Academic Press, London, 1981, p. 581.
12 M. Maja and P. Spinelli, *Werkst. Korros., 36* (1985) 554.

13 M. Schönborn and R. Aumayer, in L. J. Pearce (ed.), *Power Sources 10*, Paul Press, London, 1985, p. 537.
14 K. Kida and K. Yonezu, *Prog. Batteries Solar Cells, 4* (1982) 172.
15 A. Kita, Y. Matsumaru, M. Shinpo and H. Nakashima, in L. J. Pearce (ed.), *Power Sources 11*, International Power Sources Symposium Committee, Leatherhead, Surrey, U.K., 1986, p. 31.
16 I. K. Gibson, K. Peters and F. Wilson, in J. Thompson (ed.), *Power Sources 8*, Academic Press, London, 1981, p. 565.
17 E. M. L. Valeriote, *J. Electrochem. Soc., 128* (1981) 1423.
18 K. D. Beccu, Battelle Europe, Genève, personal communication to D. S. Carr, ILZRO, July 4, 1989.
19 E. M. L. Valeriote, J. Sklarchuck and M. S. Ho, in K. R. Bullock and D. Pavlov (eds.), *Proc. Symp. Advances in Lead–Acid Batteries*, Vol. 84-14, Electrochemical Soc. Inc., Pennington, NJ, 1984, pp. 224–240.
20 H. Tamura, H. Yoneyama, C. Iwakura and O. Ikeda, *ILZRO Project LE-254, Final Rep.*, International Lead–Zinc Research Organization, Research Triangle Park, NC, Dec. 31, 1977.
21 E. Voss, *J. Power Sources, 24* (1988) 171.
22 D. Kelly, P. Niessen and E. M. L. Valeriote, *J. Electrochem. Soc., 132* (1985) 2533.
23 H. Nakashima and S. Hattori, *Proc. Pb80, 7th Int. Lead Conf., Madrid, May 12–15, 1980*, p. 88.
24 W. C. McCrone and J. G. Delly, in *The Particle Atlas*, Vol. I, *Principles and Techniques*, Ann Arbor Science Inc., Ann Arbor, MI, 2nd edn., 1973, p. 119ff.
25 E. Voss, U. Hullmeine and A. Winsel, *J. Power Sources, 30* (1990) 33.
26 D. Pavlov and S. Ruevski, *J. Electrochem. Soc., 126* (1979) 1100.
27 H. Döring, J. Garche, W. Fischer and K. Wiesener, *J. Power Sources, 28* (1989) 367.
28 H. Döring, J. Garche, H. Dietz and K. Wiesener, *J. Power Sources, 30* (1990) 41.
29 W. G. Sunu and B. W. Burrows, in J. Thompson (ed.), *Power Sources 8*, Academic Press, London, 1981, p. 601.
30 E. Voss, *J. Power Sources, 7* (1982) 343.
31 G. Kawamura, S. Mochizuki and A. Komaki, *Denki Kagaku, 48* (1980) 554; *Prog. Batteries Solar Cells, 4* (1982) 167.
32 A. Kita, Y. Matsumaru and J. Yamashita, *Yuasa-Jiho, 58* (1985) 7.
33 J. Yamashita, H. Yufu and Y. Matsumaru, *J. Power Sources, 30* (1990) 13.
34 J. L. Weininger and E. G. Siwek, *J. Electrochem. Soc., 123* (1976) 602.
35 P. Rüetschi, *J. Electrochem. Soc., 120* (1973) 331.
36 D. Pavlov and N. Iordanov, *J. Electrochem. Soc., 117* (1970) 1103.
37 I. K. Gibson, K. Peters and F. Wilson, in J. Thompson (ed.), *Power Sources 8*, Academic Press, London, 1981, Discussion, p. 577.
38 J. Bohmann, U. Hullmeine, E. Voss and A. Winsel, *ILZRO Project LE-277, Progress Rep. No. 20 (Final Rep.)*, International Lead–Zinc Research Organization, Research Triangle Park, NC, Dec. 31, 1982.
39 U. Hullmeine, A. Winsel and E. Voss, *J. Power Sources, 25* (1989) 27.
40 U. Hullmeine, E. Voss and A. Winsel, *J. Power Sources, 30* (1990) 99.
41 D. G. Jones and D. A. J. Rand, *ILZRO Project LE-371*, proposal to International Lead–Zinc Research Organization, July 12, 1989.
42 Summary Report and Minutes of Lead-Calcium Alloy Workshop, Wantage, U.K., June 6, 1989, in *Final Rep., ILZRO Lead–Acid Battery Task Force*, Appendix D, International Lead Zinc Research Organization, Inc., Research Triangle Park, NC, Nov. 17, 1989.
43 J. S. Enochs, R. M. Meighan, C. W. Fleischmann and D. P. Boden, *Proc. 19th Ann. IECEC Conf., San Francisco, CA, Aug. 19–24, 1984*, Vol. 2, Paper No. 849287, p. 850.